Multiple transitions to chaos in a damped parametrically forced pendulum

Sang-Yoon Kim* and Kijin Lee
Department of Physics, Kangwon National University, Chunchon, Kangwon-Do 200-701, Korea
(Received 3 October 1995)

We study bifurcations associated with stability of the lowest stationary point of a damped parametrically forced pendulum by varying ω_0 (the natural frequency of the pendulum) and A (the amplitude of the external driving force). As A is increased, the stationary point will restabilize after its instability, destabilize again, and so *ad infinitum* for any given ω_0. Its destabilizations (restabilizations) occur via alternating supercritical (subcritical) period-doubling bifurcations (PDB's) and pitchfork bifurcations, except for the first destabilization, at which a supercritical or subcritical bifurcation takes place depending on the value of ω_0. For each case of the supercritical destabilizations, an infinite sequence of PDB's follows and leads to chaos. Consequently, an infinite series of period-doubling transitions to chaos appears with increasing A. The critical behaviors at the transition points are also discussed.

PACS number(s): 05.45.+b, 03.20.+i, 05.70.Jk

I. INTRODUCTION

A damped parametrically forced pendulum with a vertically oscillating support is investigated. It can be described by a second-order nonautonomous ordinary differential equation [1–3],

$$\ddot{x} + 2\pi\gamma\dot{x} + 2\pi(\omega_0^2 - A\cos 2\pi t)\sin 2\pi x = 0, \qquad (1)$$

where x is the angular position, γ the damping coefficient, ω_0 the undamped natural frequency of the unforced pendulum, and A the amplitude of the external driving force of period one. The overdot denotes the differentiation with respect to time, and all variables and parameters are expressed in dimensionless forms.

The damped parametrically forced pendulum, albeit simple looking, shows a richness in its dynamical behavior. As the amplitude A is increased to moderate values, transitions from periodic attractors to chaotic attractors and *vice versa*, coexistence of different attractors, transient chaos, and so on have been found numerically [4–6] and analytically [7]. They have also been observed in real experiments [8,9]. However, as A increases further, the damped parametrically forced pendulum exhibits interesting dynamical behaviors not found in previous works, as will be seen below.

Here we are interested in bifurcations associated with stability of the lowest stationary point with $x = 0$ and $\dot{x} = 0$ of the damped parametrically forced pendulum. The linear stability of the stationary point is determined by the linearized equation

$$\ddot{x} + 2\pi\gamma\dot{x} + 4\pi^2(\omega_0^2 - A\cos 2\pi t)x = 0, \qquad (2)$$

which is a damped Mathieu equation. For the undamped case with $\gamma = 0$, stability properties of the Mathieu equation are given in [10,11]. There exist an infinite number of disconnected instability regions of the stationary point in the ω_0-A plane. These instability regions may be called "tongues," because their lower parts are tongue shaped (see Fig. 7-5 in Ref. [11]). They can be also labeled by an integer n, since parametric resonances occur for $(\omega_0, A) = (\frac{n}{2}, 0)$. However, even a small amount of damping leads to the presence of a nonzero threshold value $A_t(n)$ of the amplitude necessary for the occurrence of the nth-order parametric resonance [1–3]. Moreover, $A_t(n)$ grows rapidly with increasing n (see Fig. 100 in Ref. [2]).

We first introduce the Poincaré map for the damped parametrically forced pendulum in Sec. II and then discuss various bifurcations associated with stability of periodic orbits. With increasing A up to sufficiently large values, the bifurcation behaviors associated with stability of the stationary point are investigated in Sec. III for a moderately damped case with $\gamma = 0.1$. The damped Mathieu equation (2) has an infinity of alternating stable and unstable A ranges for any given ω_0. Hence, as A is increased, the stationary point undergoes a cascade of "resurrections" for any given ω_0, i.e., it will restabilize after it loses its stability, destabilizes again, and so forth *ad infinitum*. Its restabilizations occur through alternationg subcritical period-doubling bifurcations (PDB's) and pitchfork bifurcations (PFB's). On the other hand, the destabilizations occur through alternating supercritical PDB's and PFB's, except for the first destabilization, at which a supercritical or subcritical bifurcation takes place, depending on the value of ω_0. For each case of the supercritical destabilizations, an infinite sequence of PDB's leading to chaos follows. Consequently, an infinite series of period-doubling transitions to chaos appears with increasing A, which was not found in previous works. This is in contrast to the cases of the one-dimensional (1D) maps and some other damped forced

*Electronic address: sykim@cc.kangwon.ac.kr

oscillators [12], in which only single period-doubling transition to chaos occurs. In Sec. IV, we study the critical scaling behaviors at the transition points. It is found that they are the same as those for the 1D maps. Finally, a summary is given in Sec. V.

II. STABILITY OF PERIODIC ORBITS, BIFURCATIONS, AND LYAPUNOV EXPONENTS IN THE POINCARÉ MAP

In this section, we first discuss stability of period orbits in the Poincaré map of the damped parametrically forced pendulum, using the Floquet theory. Bifurcations associated with the stability and Lyapunov exponents are then discussed.

The second-order ordinary differential equation (1) is reduced to two first-order ordinary differential equations:

$$\dot{x} = y, \tag{3a}$$

$$\dot{y} = -2\pi\gamma y - 2\pi(\omega_0^2 - A\cos 2\pi t)\sin 2\pi x. \tag{3b}$$

The Poincaré maps of an initial point $z_0[\equiv (x(0), y(0))]$ can be computed by sampling the points z_m at the discrete time $t = m$, where $m = 1, 2, 3, \ldots$. We call the transformation $z_m \to z_{m+1}$ the Poincaré (time-1) map, and write $z_{m+1} = P(z_m)$.

The Poincaré map P has an inversion symmetry such that

$$SPS(z) = P(z) \text{ for all } z, \tag{4}$$

where $z = (x, y)$, S is the inversion of z, i.e., $S(z) = -z$. If an orbit $\{z_m\}$ of P is invariant under S, then it is called a symmetric orbit. Otherwise, it is called an asymmetric orbit and has its "conjugate" orbit $S\{z_m\}$.

We now study the stability of a periodic orbit with period q such that $P^q(z_0) = z_0$ but $P^j(z_0) \neq z_0$ for $1 \leq j \leq q-1$. Here P^k means the k-times iterated map. The linear stability of the q-periodic orbit is determined from the linearized-map matrix $DP^q(z_0)$ of P^q at an orbit point z_0. Using the Floquet theory [13], the matrix DP^q can be obtained by integrating the linearized differential equations for small perturbations as follows.

Let $z^*(t) = z^*(t+q)$ be a solution lying on the closed orbit corresponding to the q-periodic orbit. In order to determine the stability of the closed orbit, we consider an infinitesimal perturbation $[\delta x(t), \delta y(t)]$ to the closed orbit. Linearizing Eq. (3) about the closed orbit, we obtain

$$\begin{pmatrix} \delta\dot{x} \\ \delta\dot{y} \end{pmatrix} = J(t) \begin{pmatrix} \delta x \\ \delta y \end{pmatrix}, \tag{5}$$

where

$$J(t) = \begin{pmatrix} 0 & 1 \\ -4\pi^2(\omega_0^2 - A\cos 2\pi t)\cos 2\pi x^*(t) & -2\pi\gamma \end{pmatrix}. \tag{6}$$

Note that J is a 2×2 q-periodic matrix. Let $W(t) = [w^1(t), w^2(t)]$ be a fundamental solution matrix with $W(0) = I$. Here $w^1(t)$ and $w^2(t)$ are two independent solutions expressed in column vector forms and I is the 2×2 unit matrix. Then a general solution of the q-periodic system has the following form:

$$\begin{pmatrix} \delta x(t) \\ \delta y(t) \end{pmatrix} = W(t) \begin{pmatrix} \delta x(0) \\ \delta y(0) \end{pmatrix}. \tag{7}$$

Substitution of Eq. (7) into Eq. (5) leads to an initial-value problem in determining $W(t)$:

$$\dot{W}(t) = J(t)W(t), \quad W(0) = I. \tag{8}$$

It is clear from Eq. (7) that $W(q)$ is just the linearized-map matrix $DP^q(z_0)$. Hence the matrix DP^q is calculated through integration of Eq. (8) over the period q.

The characteristic equation of the linearized-map matrix M (precisely equal to DP^q) is

$$\lambda^2 - \mathrm{tr}M\,\lambda + \det M = 0, \tag{9}$$

where $\mathrm{tr}M$ and $\det M$ denote the trace and determinant of M, respectively. The eigenvalues, λ_1 and λ_2, of M are called the Floquet stability multipliers. As shown in [14], $\det M$ is calculated from a formula

$$\det M = e^{\int_0^q \mathrm{tr}\,J dt}. \tag{10}$$

Substituting the trace of M (i.e., $\mathrm{tr}J = -2\pi\gamma$) into Eq. (10), we obtain

$$\det M = e^{-2\pi\gamma q}. \tag{11}$$

Hence, the Poincaré map P is a two-dimensional (2D) dissipative map with a constant Jacobian determinant (less than unity), like the Hénon map [15].

The pair of stability multipliers of a periodic orbit lies either on the circle of radius $e^{-\pi\gamma q}$ or on the real axis in the complex plane. The periodic orbit is stable only when both multipliers lie inside the unit circle. We first note that they never cross the unit circle and hence Hopf bifurcations do not occur. Consequently, it can lose its stability only when a multiplier decreases (increases) through -1 (1) on the real axis.

A more convenient real quantity R, called the residue and defined by

$$R \equiv \frac{1 + \det M - \mathrm{tr}M}{2(1 + \det M)}, \tag{12}$$

was introduced in [16] to characterize stability of periodic orbits in 2D dissipative maps with constant Jacobian determinants. A periodic orbit is stable when $0 < R < 1$; at both ends of $R = 0$ and 1, the stability multipliers λ are 1 and -1, respectively. When R decreases through 0 (i.e., λ increases through 1), the periodic orbit loses its stability via saddle-node or pitchfork or transcritical bifurcation. On the other hand, when R increases through 1 (i.e., λ decreases through -1), it becomes unstable via PDB, also referred to as a flip or subharmonic bifurcation. For each case of the PFB's and PDB's, two types of supercritical and subcritical bifurcations occur. For

more details on bifurcations, refer to Ref. [17].

Lyapunov exponents of an orbit $\{z_m\}$ in the Poincaré map P characterize the mean exponential rate of divergence of nearby orbits [18]. There exist two Lyapunov exponents σ_1 and σ_2 ($\sigma_1 \geq \sigma_2$) such that $\sigma_1+\sigma_2 = -2\pi\gamma$, because the linearized Poincaré map DP has a constant Jacobian determinant, $\det DP = e^{-2\pi\gamma}$. We choose an initial perturbation δz_0 to the initial orbit point z_0 and iterate the linearized map DP for δz along the orbit to obtain the magnitute d_m ($\equiv |\delta z_m|$) of δz_m. Then, for almost all infinitesimally small initial perturbations, we have the largest Lyapunov exponent σ_1 given by

$$\sigma_1 = \lim_{m\to\infty} \frac{1}{m} \ln \frac{d_m}{d_0}. \tag{13}$$

If σ_1 is positive, then the orbit is called a chaotic orbit; otherwise, it is a regular orbit.

III. MULTIPLE PERIOD-DOUBLING TRANSITIONS TO CHAOS

In this section, by varying two parameters ω_0 and A, we study bifurcations associated with stability of the stationary point of the damped parametrically forced pendulum for a moderately damped case with $\gamma = 0.1$. It is found that with increasing A, the stationary point undergoes an infinite series of period-doubling transitions to chaos for any given ω_0. This is in contrast to the 1D maps and some other damped forced oscillators [12] with only single period-doubling transition to chaos.

The stability diagram of the stationary point is given in Fig. 1. There exist an infinity of disconnected instability regions in the ω_0-A plane, which are separated by one connected stability region. The instability regions may be called tongues, because their lower parts are tongue shaped. They can be also labeled by an integer n since, for the undamped case of $\gamma = 0$, parametric resonances occur at $(\omega_0, A) = (\frac{n}{2}, 0)$ [1–3,10,11]. However, even a small amount of damping results in a nonzero minimal value $A_t(n)$ of the amplitude necessary for the occurrence of the nth-order parametric resonance [1–3]. Furthermore, $A_t(n)$ grows rapidly with increasing n (see Fig. 1). Hereafter, each tongue of order n is denoted by T_n.

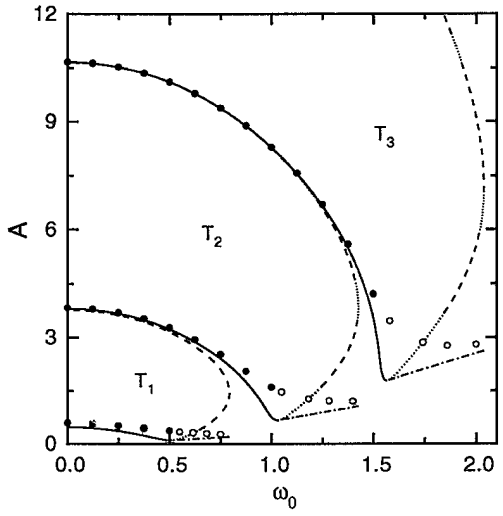

FIG. 1. Stability diagram of the stationary point of the damped parametrically forced pendulum. There exist an infinity of tongues T_n of instability regions. For each tongue, a supercritical bifurcation occurs on the solid boundary curve, whereas a subcritical bifurcation takes place on the remaining dashed or short-dotted boundary curve. There are also saddle-node-bifurcation curves touching the tongue boundaries, which are denoted by the dash-dotted curves. The accumulation points of PDB's, denoted by solid and open circles, form critical lines. For other details, see the text.

With increasing A, each tongue T_n is twisted to the left, and lies above the tongue T_{n-1}. In this way, tongues pile up successively, as shown in Fig. 1. Consequently, there exist an infinity of alternating stable and unstable A ranges for any given ω_0. Hence, as A is increased, the stationary point will restabilize after it loses its instability, destabilize again, and so forth *ad infinitum* for any given ω_0. Such "resurrection" mechanisms are given below.

Bifurcation behaviors at the tongue boundaries are investigated in detail. They depend on whether the tongue order n is odd or even. At the tongue boundaries of odd (even) order n, the residue of the stationary point is 1 (0). Consequently, PDB's and PFB's occur when tongue boundaries of odd and even order n are crossed, respectively. For example, the boundaries of T_1 and T_3 in Fig. 1 are PDB curves, while the boundary of T_2 is a PFB curve. For the cases of PDB's and PFB's, there are two types of supercritical and subcritical bifurcations, which occur depending on where tongue boundaries are crossed. A saddle-node bifurcation curve, at which a pair of stable and unstable orbits with period 2 (1) is born, touches each tongue boundary of odd (even) order n at a boundary point $[\omega_b(n), A_b(n)]$, and decomposes it into the supercritical and subcritical parts. As an example, see the three saddle-node-bifurcation curves, denoted by dash-dotted curves, touching the boundaries of T_1, T_2, and T_3 in Fig. 1. On the lower left-hand part of each tongue boundary, denoted by a solid curve, a supercritical bifurcation occurs. The remaining subcritical boundary curve starting from $[\omega_b(n), A_b(n)]$ first goes to the right, but then turns left at a point $[\omega_t(n), A_t(n)]$. It consists of two types of subparts, denoted by short-dotted and dashed curves, on which a subcritical bifurcation takes place. On the subcritical segment with $\omega_b(n) < \omega_0 < \omega_t(n)$, the stationary point absorbs an unstable orbit born at a dash-dotted saddle-node-bifurcation curve and loses its stability. On the other hand, the stable orbit born by the same saddle-node bifurcation undergoes an infinite series of PDB's leading to chaos. The accumulation points of such PDB's are denoted by open circles in Fig. 1.

When the stationary point loses its stability via supercritical PDB's and PFB's, the system is asymptotically attracted to periodic attractors (born by the supercritical bifurcations) with the doubled period and the same period, respectively. However, for the subcritical bifurcation cases, the asymptotic states just after the instability of the stationary point may be periodic or chaotic, depending on which subparts of the subcritical boundaries are crossed. In Fig. 2, we fix different ω_0

and increase A to cross different subparts of a subcritical boundary of T_1. When a short-dotted boundary curve is crossed, the asymptotic state becomes periodic [see Fig. 2(a)], because the stationary point jumps to a periodic attractor born by a saddle-node bifurcation after its instability. For this periodic case, with increasing A an infinite sequence of supercritical PDB's leading to small-scale chaos follows. However, when a dashed boundary is crossed, large-scale full chaos appears via intermittency [19], and hence the asymptotic state becomes chaotic [see Fig. 2(b)].

With increasing A, up to sufficiently large values, the bifurcation behaviors associated with stability of the stationary point are investigated in detail for many values of ω_0. For a given ω_0, the restabilizations of the stationary point occur via alternating subcritical PDB's and PFB's with increasing A, as shown in Fig. 1. On the other hand, the destabilizations take place via alternating supercritical PDB's and PFB's, except for the first destabilization,

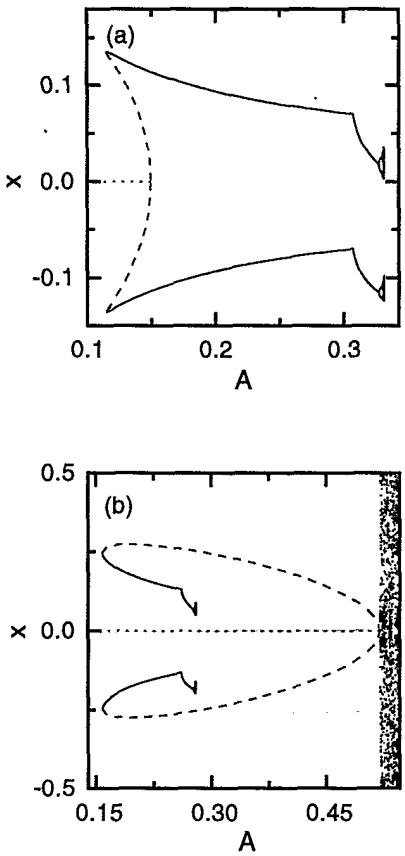

FIG. 2. Asymptotic states after the instability of the stationary point via subcritical bifurcations. A pair of symmetric stable and unstable orbits of period 2 is born via saddle-node bifurcation. The x-positions of the stable and unstable orbits are denoted by the solid and dashed curves, respectively. At a subcritical PDB point, the stationary point, whose x-position is denoted by the dotted line, loses its stability by absorbing the unstable 2-periodic orbit. After its instability, (a) the stationary point jumps to the stable 2-perodic orbit for $\omega_0 = 0.55$, whereas (b) large-scale full chaos appears for $\omega_0 = 0.6832$. Note also that for each case, the stable 2-periodic orbit undergoes an infinite sequence of PDB's leading to small-scale chaos.

at which a supercritical or subcritical bifurcation occurs depending on the value of ω_0 [e.g., for $\omega_0 = 0.5$ (0.65), the first destabilization occurs via supercritical (subcritical) PDB]. For each case of the supercritical destabilizations, an infinite sequence of supercritical PDB's leading to a pair of chaotic attractors follows and ends at a finite accumulation point. In each tongue, such accumulation points of PDB's, denoted by solid circles in Fig.1, seem to form a smooth critical line. Consequently, an infinite series of period-doubling transitions to chaos appears with increasing A. This is in contrast to the cases of the 1D maps and some other damped forced oscillators [12], in which only single period-doubling transition to chaos occurs.

As an example of the multiple period-doubling transitions to chaos, consider the case $\omega_0 = 0.5$. A bifurcation diagram along the vertical line $\omega_0 = 0.5$ is shown in Fig. 3. Through a supercritical PDB, the stationary point loses its stability at its first destabilization point $A_d(1) = 0.100\,218\ldots$, and a symmetric orbit of period 2 is born. Unlike the case of the stationary point, the symmetric 2-periodic orbit becomes unstable by a symmetry-breaking supercritical PFB, which leads to the birth of a conjugate pair of asymmetric orbits with period 2. (For the sake of convenience, only one asymmetrical orbit of period 2 is shown in Fig. 3 [20].) However, as A is further increased, an infinite sequence of supercritical PDB's follows and ends at its accumulation point A_1^* ($0.357\,709\,84\ldots$). The critical scaling behaviors of period doublings near the critical point A_1^* are the same as those for the 1D maps, as will be seen in Sec. IV.

After the period-doubling transition to chaos, a conjugate pair of small chaotic atttractors with positive largest Lyapunov exponent σ_1 appear. As A is increased, the different parts of a chaotic attractor coalesce and form larger pieces. For example, the chaotic attractor with $\sigma_1 \simeq 0.091$ shown in Fig. 4(a) seems to be composed

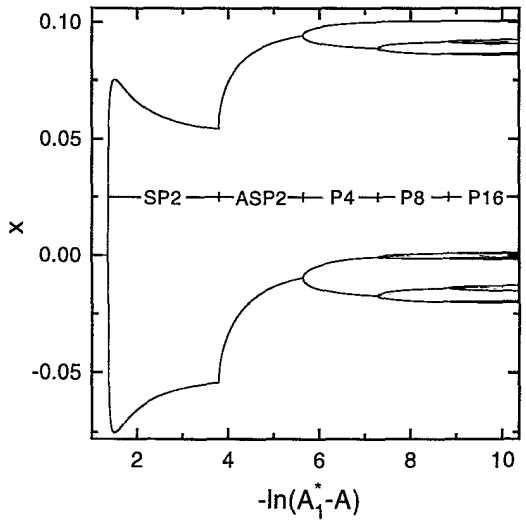

FIG. 3. First bifurcation diagram for $\omega_0 = 0.5$. SP2 and ASP2 denote the stable A ranges of the symmetric and asymmetric orbits of period 2, respectively. PN also designates the stable A range of the asymmetric periodic orbit with period N ($N = 4, 8, 16$).

of four distinct pieces for $A = 0.3579$. As shown in Fig. 4(b), these pieces coalesce to form two large pieces with $\sigma_1 = 0.158$ for $A = 0.3582$. However, beyond some critical point $A_c(1)$ ($\simeq 0.3586$), the chaotic attractor becomes unstable, and the system is asymptotically attracted to a rotational orbit of period 1 born by a saddle-node bifurcation. For $A > A_c(1)$, the damped parametrically forced pendulum continues to exhibit rich dynamical behaviors. With increasing A, the birth of new periodic attractors via saddle-node bifurcations, transitions from periodic attractors to chaotic attractors and *vice versa*, coexistence of different attractors, and so on are found until the stationary point restabilizes. (For more details on such dynamical behaviors, refer to previous works [4–9].) However, with further increasing A, the damped parametrically forced pendulum exhibits interesting dynamical behaviors not previously found.

When the dashed subcritical boundary of T_1 is crossed at the first restabilization point $A_r(1)$ (3.150 509 ...), the stationary point restabilizes via subcritical PDB. An "inverse" process of the case of Fig. 2(b) occurs. There exists large-scale full chaos below $A_r(1)$. When A increases through $A_r(1)$, the large chaotic attractor disappears and the restabilization of the stationary point occurs with birth of a new unstable 2-periodic orbit. The residue R of the stationary point decreases monotonically from one and becomes zero at the second destabilization point $A_d(2)$ (3.224 230 ...) on the supercritical PFB curve of T_2.

A second bifurcation diagram for $\omega_0 = 0.5$ is shown in Fig. 5. The stationary point becomes unstable via symmetry-breaking supercritical PFB at its second destabilization point $A_d(2)$, which results in the birth of a conjugate pair of asymmetric orbits with period 1. With further increase of A, a second infinite sequence of supercritical PDB's follows and ends at its accumulation point A_2^* (3.263 703 15 ...). The critical scaling behaviors of period doublings near $A = A_2^*$ are the same as those near the first accumulation point A_1^*. After the second period-doubling transition to chaos, a conjugate pair of small chaotic attractors also appears. They persist until some critical point $A_c(2)$ ($\simeq 3.263\,862$) beyond which the system is asymptotically attracted to an oscillating 2-periodic orbit born via saddle-node bifurcation. As in the tongue of order 1, the damped parametrically forced pendulum exhibits diverse dynamical behaviors such as transitions between the periodic and chaotic attractors and the coexistence of different attractors in the region between $A_c(2)$ and the second restabilization point $A_r(2)$ (10.093 985 ...).

When the dashed subcritical boundary of T_2 is crossed at $A_r(2)$, a subcritical PFB occurs. Consequently, the stationary point restabilizes with the birth of a pair of new unstable orbits of period 1. As A is further increased, the residue R of the stationary point monotonically increases and becomes one at the third destabilization point $A_d(3)$ (10.097 583 ...) on the supercritical PDB curve of T_3. Since the order of T_3 is odd, the subsequent bifurcation behaviors in T_3 are the same as those for the case of T_1. That is, a third infinite sequence of supercritical PDB's, leading to a pair of small chaotic attractors, follows and ends at its accumulation point A_3^* (10.099 660 93 ...). This third bifurcation diagram for

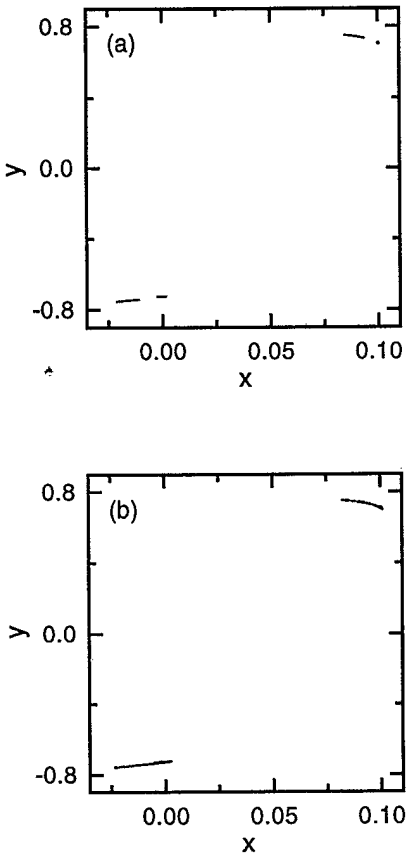

FIG. 4. Chaotic attractors after the first period-doubling transition to chaos. (a) For $A = 0.3579$, the chaotic attractor with the largest Lyapunov exponent $\sigma_1 \simeq 0.091$ is composed of four pieces. (b) These pieces merge to form two large pieces with $\sigma_1 \simeq 0.158$ for $A = 0.3582$.

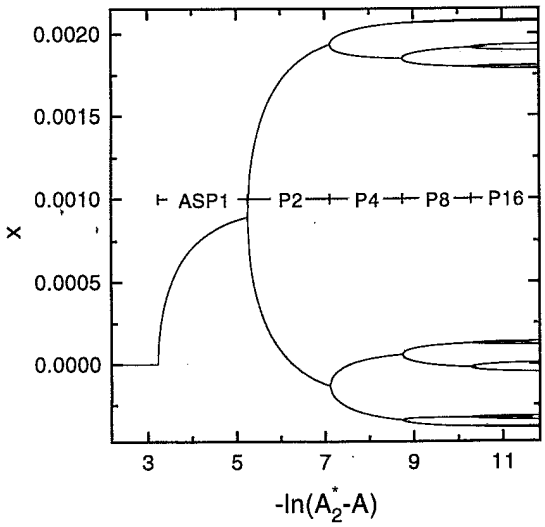

FIG. 5. Second bifurcation diagram for $\omega_0 = 0.5$. ASP1 and PN denote the stable A ranges of the asymmetric orbit of period 1 and N ($N = 2, 4, 8, 16$), respectively.

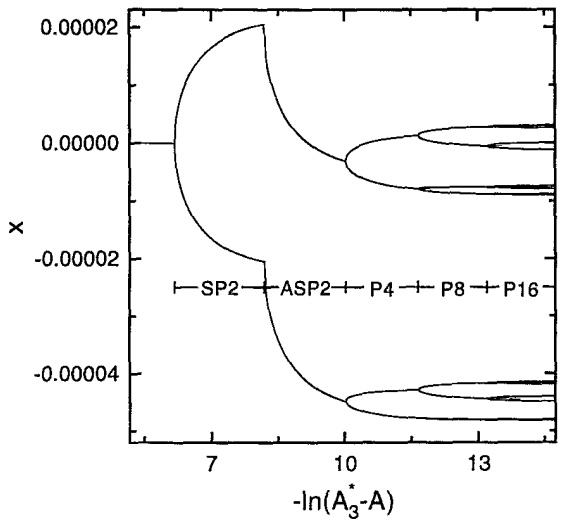

FIG. 6. Third bifurcation diagram for $\omega_0 = 0.5$. SP2 and ASP2 denote the stable A ranges of the symmetric and asymmetric orbits of period 2, respectively. The PN also designates the stable A range of the asymmetric periodic orbit with period $N(N = 4, 8, 16)$.

$\omega_0 = 0.5$ is given in Fig. 6. The critical scaling behaviors of period doublings near A_3^* are also the same as those near A_1^*, as will be seen in the next section.

We have also studied many other cases with different ω_0, and found multiple period-doubling transitions to chaos with increasing A. Such accumulation points are denoted by solid circles in Fig. 1. In each tongue of order n, they form a smooth critical line $A_n^*(\omega_0)$. Since the range of ω_0 is $0 < \omega_0 < \omega_b(n)$, each critical line of order n ends inside the tongue with order n. As mentioned above, a stable periodic orbit, born at a dash-dotted saddle-node-bifurcation curve, also undergoes an infinite sequence of supercritical PDB's. The accumulation points of such PDB's, denoted by open circles in Fig. 1, form another critical line. The two different critical lines join at a point with $\omega_0 = \omega_b(n)$. Consequently, each critical line of order n extends to the outside of the tongue of order n.

IV. CRITICAL BEHAVIORS OF PERIOD-DOUBLING BIFURCATIONS

In this section, we study the critical behaviors of PDB's for many values of ω_0. The orbital scaling behavior and the power spectra of the periodic orbits born via PDB's as well as the parameter scaling behavior are particularly investigated. The critical behaviors for all cases studied are found to be the same as those for the 1D maps.

As an example, we consider the case $\omega_0 = 0.5$. The first three period-doubling transition points A_i^*'s $(i = 1, 2, 3)$ are shown in Fig. 1. Only the critical behaviors near A_1^* are given below, because the critical behaviors at the three transition points are the same. For this case, we follow the periodic orbits of period 2^k up to level $k = 8$. As explained above, for $A = A_d(1)$, the stationary point becomes unstable via supercritical PDB and a new symmetric 2-periodic orbit appears (see Fig. 3). However, the symmetric orbit of period 2 loses its stability by a symmetry-breaking supercritical PFB at $A = 0.335\,257\ldots$. As a result, a conjugate pair of asymmetric 2-periodic orbits appears. As A is further increased, each asymmetrical orbit with period 2 undergoes an infinite sequence of supercritical PDB's, ending at its accumulation point A_1^*. Table I gives the A values at which the supercritical PDB's take place; at A_k, the residue R_k of an asymmetric orbit of period 2^k is one. The sequence of A_k converges geometrically to its limit value A_1^* with an asymptotic ratio δ:

$$\delta_k = \frac{A_k - A_{k-1}}{A_{k+1} - A_k} \to \delta. \tag{14}$$

The sequence of δ_k is also listed in Table I. Note that its limit value δ ($\simeq 4.67$) agrees well with that (4.669...) for a 1D map $x_{m+1} = f(x_m)$ with a single quadratic maximum x^* [21]. We also obtain the value of A_1^* (0.357 709 845 3) by superconverging the sequence of $\{A_k\}$ [22].

For the 1D map f, consider a 2^k-periodic orbit point $x^{(k)}$ nearest to the maximum point x^* when the orbit becomes unstable. Then, the sequence of $x^{(k)}$ also converges geometrically to the maximum point x^* with an asymptotic ratio $\alpha = -2.502\ldots$ [21]. Note that the region near the maximum point x^* is the most rarified region, because the distance between $x^{(k)}$ and its nearest orbit point $f^{2^{k-1}}(x^{(k)})$ is maximum. Hence, for the case of the Poincaré map P, we first locate the most rari-

TABLE I. Asymptotically geometric convergence of the parameter values for successive supercritical PDB's from an asymmetric 2-periodic orbit.

k	A_k	δ_k
1	0.354 163 288 011	
2	0.357 022 317 174	5.286
3	0.357 563 141 135	4.692
4	0.357 678 400 212	4.665
5	0.357 703 107 281	4.666
6	0.357 708 401 983	4.668
7	0.357 709 536 272	4.670
8	0.357 709 779 136	

TABLE II. Asymptotically geometric convergence of the orbital sequences $\{x^{(k)}\}$ and $\{y^{(k)}\}$.

k	$x^{(k)}$	$\alpha_{x,k}$	$y^{(k)}$	$\alpha_{y,k}$
1	0.094 410 516		0.719 956 679	
2	0.088 901 931	-1.933	0.738 357 722	-3.935
3	0.091 750 680	-3.085	0.733 681 177	-2.156
4	0.090 827 396	-2.261	0.735 850 056	-2.717
5	0.091 235 660	-2.635	0.735 051 829	-2.398
6	0.091 080 705	-2.436	0.735 384 746	-2.558
7	0.091 144 315	-2.538	0.735 254 611	-2.474
8	0.091 119 256		0.735 307 206	

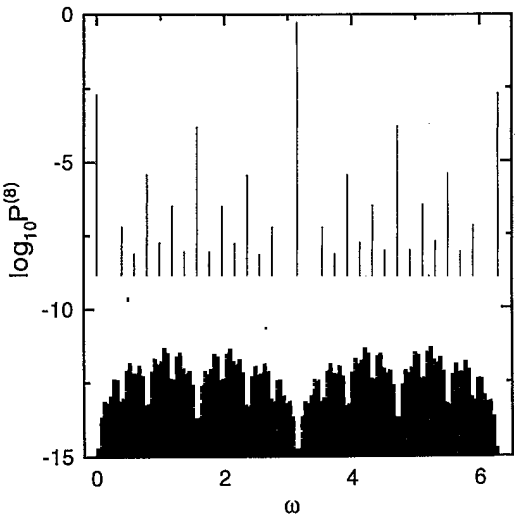

FIG. 7. Plot of $\log_{10}P^{(8)}$ vs (ω) for $A = A_8$ (0.357 709 779 136).

fied region by choosing an orbit point $z^{(k)}$ $[= (x^{(k)}, y^{(k)})]$ that has the largest distance from its nearest orbit point $P^{2^{k-1}}(z^{(k)})$ for $A = A_k$. The two sequences $\{x^{(k)}\}$ and $\{y^{(k)}\}$ are listed in Table II. Note that they converge geometrically to their limit values x^* and y^* with the 1D asymptotic ratio α, respectively,

$$\alpha_{x,k} = \frac{x^{(k)} - x^{(k-1)}}{x^{(k+1)} - x^{(k)}} \to \alpha, \quad \alpha_{y,k} = \frac{y^{(k)} - y^{(k-1)}}{y^{(k+1)} - y^{(k)}} \to \alpha. \tag{15}$$

The values of x^* (0.091 126) and y^* (0.735 292) are also obtained by superconverging the sequences of $x^{(k)}$ and $y^{(k)}$, respectively.

We also study the power spectra of the 2^k-periodic orbits $(k = 1, \ldots, 8)$ at the PDB points A_k. Consider the orbit of level k whose period is $q = 2^k$, $[z_m^{(k)} = (x_m^{(k)}, y_m^{(k)})$, $m = 0, 1, \ldots, q-1]$. Then, the jth Fourier component of this 2^k-periodic orbit is given by

$$z^{(k)}(\omega_j) = \frac{1}{q}\sum_{m=0}^{q-1} z_m^{(k)} e^{-i\omega_j m}, \tag{16}$$

where $\omega_j = 2\pi j/q$, and $j = 0, 1, \ldots, q-1$. The power spectrum $P^{(k)}(\omega_j)$ of level k defined by

$$P^{(k)}(\omega_j) = |z^{(k)}(\omega_j)|^2 \tag{17}$$

has discrete peaks at $\omega = \omega_j$. In the power spectrum of the next $(k+1)$ level, new peaks of the $(k+1)$th generation appear at odd harmonics of the fundamental frequency, $\omega_j = 2\pi(2j+1)/2^{(k+1)}$ $(j = 0, \ldots, 2^k - 1)$. To classify the contributions of successive PDB's in the power spectrum of level k, we write

TABLE III. Sequence $2\beta^{(k)}(l)$ $[\equiv \phi^{(k)}(l)/\phi^{(k)}(l+1)]$ of the ratios of the successive average heights.

k	l				
	3	4	5	6	7
6	19.8	22.5	21.1		
7	19.8	22.1	21.2	21.5	
8	19.8	22.0	20.7	21.6	21.4

$$P^{(k)} = P_{00}\delta(\omega) + \sum_{l=1}^{k}\sum_{j=0}^{2^{(l-1)}-1} P_{lj}^{(k)}\delta(\omega - \omega_{lj}), \tag{18}$$

where $P_{lj}^{(k)}$ is the height of the jth peak of the lth generation appearing at $\omega = \omega_{lj}$ $[2\pi(2j+1)/2^l]$. As an example, see the power spectrum $P^{(8)}(\omega)$ of level 8 shown in Fig. 7. The average height of the peaks of the lth generation is given by

$$\phi^{(k)}(l) = \frac{1}{2^{(l-1)}}\sum_{j=0}^{2^{l-1}-1} P_{lj}^{(k)}. \tag{19}$$

Whether or not the sequence of the ratios of the successive average heights

$$2\beta^{(k)}(l) = \phi^{(k)}(l)/\phi^{(k)}(l+1), \tag{20}$$

converges is of interest. The ratios are listed in Table III. They seem to approach a limit value $2\beta \simeq 21$ that agrees well with that (20.96...) for the 1D map [23].

V. SUMMARY

Bifurcations associated with stability of the stationary point of the damped parametrically forced pendulum are investigated by varying two parameters ω_0 and A. As A is increased, the stationary point undergoes an infinite sequence of alternating restabilizations and destabilizations for any given ω_0. The restabilization and destabilization mechanisms are also given in detail. We find that an infinite series of period-doubling transitions to chaos appears with increasing A. To our knowledge, this was not found in previous works. This is in contrast to the cases of the 1D maps and some other damped forced oscillators [12] with only single period-doubling transition. The critical scalings at the transition points are also found to be the same as those of the 1D maps.

ACKNOWLEDGMENTS

This work was supported by the Basic Science Research Institute Program, Ministry of Education, Korea, Project No. BSRI-95-2401.

[1] L.D. Landau and E.M. Lifshitz, *Mechanics* (Pergamon Press, New York, 1976), p. 80.
[2] V.I. Arnold, *Mathematical Methods of Classical Mechanics* (Springer-Verlag, New York, 1978), p. 113.
[3] V.I. Arnold, *Ordinary Differential Equations* (MIT Press, Cambridge, 1973), p. 203.
[4] J.B. McLaughlin, J. Stat. Phys. **24**, 375 (1981).
[5] R.W. Leven and B.P. Koch, Phys. Lett. A **86**, 71 (1981).
[6] A. Arneodo, P. Coullet, C. Tresser, A. Libchaber, J. Maurer, and D. d'Humières, Physica D **6**, 385 (1983).
[7] B.P. Koch and R.W. Leven, Physica D **16**, 1 (1985).
[8] B.P. Koch, R.W. Leven, B. Pompe, and C. Wilke, Phys. Lett. A **96**, 219 (1983).
[9] R.W. Leven, B. Pompe, C. Wilke, and B.P. Koch, Physica D **16**, 371 (1985).
[10] P.M. Morse and H. Feshbach, *Methods of Theoretical Physics* (McGraw-Hill, New York, 1953), Sec. 5.2.
[11] J. Mathews and R.L. Walker, *Mathematical Methods of Physics* (Benjamin, New York, 1965), Sec. 7.5.
[12] T. Kai, Phys. Lett. A **86**, 263 (1981); J. Testa, J. Perez, and C. Jeffries, Phys. Rev. Lett. **48**, 714 (1982).
[13] S. Lefschetz, *Differential Equations: Geometric Theory* (Dover Publications, Inc., New York, 1977), Sec. 3.5.
[14] S. Lefschetz, *Differential Equations: Geometric Theory* (Dover Publications, Inc., New York, 1977), p. 60.
[15] M. Hénon, Commun. Math. Phys. **50**, 69 (1976).
[16] S.-Y. Kim and B. Hu, Phys. Rev. A **44**, 934 (1991); S.-Y. Kim and D.-S. Lee, Phys. Rev. A **45**, 5480 (1992).
[17] J. Gukenheimer and P. Holmes, *Nonlinear Oscillations, Dynamical Systems, and Bifurcations of Vector Fields* (Springer-Verlag, New York, 1983), Sec. 3.5.
[18] A.J. Lichtenberg and M.A. Lieberman, *Regular and Stochastic Motion* (Springer-Verlag, New York, 1983), Sec. 5.3.
[19] Y. Pomeau and P. Manneville, Commun. Math. Phys. **74**, 189 (1980); A. Lahiri and T. Nag, Phys. Rev. Lett. **62**, 1933 (1989).
[20] For each asymmetric case, only one of the two conjugate asymmetric orbits is shown in a bifurcation diagram or in the phase plane.
[21] M.J. Feigenbaum, J. Stat. Phys. **19**, 25 (1978); **21**, 669 (1979).
[22] R. S. MacKay, Ph.D. thesis, Princeton University, 1982. See Eqs. 3.1.2.12 and 3.1.2.13.
[23] M. Nauenberg and J. Rudnick, Phys. Rev. B **24**, 493 (1981).